2007 American WJTA Conference and Expo
August 19-21, 2007 • Houston, Texas

Paper

THE CHARACTERIZATION OF ROCK FAILURE INDUCED BY HIGH FREQUENCY MODULATED FLUID JETS IN CRYSTALLINE ROCK

H. B. Miller
Colorado School of Mines
Golden, Colorado, USA

F.D. Wang
International Engineering Technology, Inc.
Golden, Colorado, USA

ABSTRACT

High frequency, spatially discrete fluid masses that are formed in free-stream by varying the impedance of a continuous flow describe the basic premise of a percussive jet. Due to their dynamic characteristics and success in fragmenting rock, these jets may represent a viable alternative to conventional excavation methods in select hardrock applications.

This paper presents the results of an investigation into the empiric relationships between system parameters and the mode of failure observed in crystalline rock. The study confirms long held suspicions that the failure mechanisms associated with percussive jet impingement are wholly different than those attributed to continuous waterjets for the rock type tested. As observed, failure was dominated by the extension and coalescence of tensile fractures through hydraulic pressurization and dynamic loading, where erosional mechanisms played only an ancillary role. Often pervasive, surface spalling proved to be highly dependent upon traverse velocity. The influence of exposed fractures along rock surfaces and in the kerf was shown to benefit excavation efficiency, particularly at lower traverse speeds. As traverse velocities increased, the mode of failure appeared to become increasingly less dependent upon subsurface fluid penetration and more reliant on differential loading, elastic compression, and surface scouring.

Organized and Sponsored by the WaterJet Technology Association

INTRODUCTION

The continuing fascination with nontraditional excavating technologies in hardrock applications, such as mining, tunneling, and underground heavy construction, has largely been driven by the limitations associated with the current generation of mining systems and mechanical excavators. Whether it be by the traditional unit operations of drill and blast or excavators employing direct contact tools, there exist economic and physical disincentives to their use in an increasing number of applications. These constraints stem from the inherent operating and mechanical characteristics of these systems, their limited scope of economic application, and the size of projects necessary to financially facilitate their utilization. These obstacles are inordinately apparent in labor intensive applications involving confined space excavation, such as those found in urban construction and the mining of tabular deposits. In these operating environments, there are tremendous economic incentives to employing rapid and continuous excavating methods that are capable of producing non-circular openings in hardrock formations through remote and/or tele-robotic control. Unfortunately, in these applications, there are presently few alternatives that are both technically feasible and economically viable.

The breadth of these novel excavation technologies spans a wide diversity of mechanisms embracing countless mechanical and chemical processes. Of the systems that have received serious attention, none presents greater near-term opportunities for substantive advancement in underground excavating systems than does waterjet technology. The term “waterjet technology” actually comprises a wide spectrum of different techniques and equipment designs, each possessing distinctive hydrodynamic and impingement characteristics. By their nature, waterjets differ from conventional excavation methods in physical design, operation, and mode of fragmentation. In many applications, waterjets possess inherent advantages over blasting methods and mechanical tools. Foremost amongst these beneficial attributes include; no direct mechanical contact between the nozzle assemble and the rock surface, the ability to orient the jet at virtually any angle without appreciable losses in power, the amenability of waterjets for remote control and automation, the degree of flexibility associated with system integration and the ability to adapt to changing operating conditions, the absence of dust or gases, and the amount of energy that can be selectively focused over very small target areas.

Despite these advantages, technical constraints exist that have economically impeded the commercialization of waterjet excavation systems in most hardrock mining and construction applications. Paramount among these challenges is the low energy efficiency associated with volumetric removal, limited standoff distance, the relatively low rate of production, and the size distribution of the liberated cuttings. To circumvent these constraints, researchers have investigated a multitude of strategies, equipment configurations, and alternative waterjet technologies. While significant strides have been made and many of these research efforts have achieved some measure of success in specific applications, the economic utility of waterjet excavation systems designed for use in hardrock applications have thus far failed to demonstrate a level of performance necessary to achieve industry acceptance.

Percussive (Modulated) Waterjets

The ability to generate high frequency, spatially quasi-discrete fluid masses by varying the flow impedance of a positively discharged, continuous waterjet is the basic premise which defines a percussive jet. While the jet is continuously discharged from a conventional orifice with a constant momentum flux, modulation of the flow prior to nozzle acceleration induces dynamic changes in the fluid characteristics that result in free-stream variations of the jet's cross-sectional area as a function of time and distance. Modulation is accomplished by cycling the discharge flow rate above and below its average at some predetermined amplitude, frequency, and waveform. As a consequence, individual unit volumes within each discharge cycle have different axial velocities, in which the fast and slow portions of each cycle coalesce in free-stream (Figure 1). This convergence causes periodic fluid masses, commonly referred to as bunches, to form within the stream that can eventually separate into discrete pulses.

The dynamic behavior of percussive modulated flows is novel and differentiates it from other waterjet technologies that employ pulsed, intermittent, or disrupted stream flows. Foremost among these unique characteristics is the capability to exercise definitive control over the processes believed to be responsible for bunch formation, structure, and dynamic composition. Such control implies the ability to optimize the aerodynamic and impact properties of individual fluid pulses entrained within the free-stream relative to a specific rock type or to facilitate a desired target response. The innate proficiency of these jets to fragment hard crystalline rocks and other brittle materials has been the driving force behind this and related studies.

Research of these innovative jet flows is truly in its infancy, where pragmatic investigations into the mechanics of modulation and free-stream dynamics is fairly limited in both theoretical scope and empirical study. Furthermore, the processes associated with bunch impingement and material failure are extremely complex and difficult to quantify. To facilitate technical advances in the physical design of these systems to the level necessary for commercial application, a comprehensive understanding of these enigmatic multifaceted mechanisms is essential. In this pursuit, the primary objective of this work has been to identify and characterize the principle failure mechanisms related to the impingement of percussive modulated jets against select types of brittle rocks and geomaterials.

History of Jet Development

Developed by Dr. Eugene Nebeker of Scientific Associates, Inc. (SAI), the concept of percussive waterjets was prompted by research into the combustion stability of modulated liquid propellants in rocket engines. In 1973, SAI conducted a preliminary investigation of this technology for the U.S. Army Mobility Equipment Research and Development Center with the expressed objectives of assessing the technical feasibility of generating percussive jet flows and their potential utility in rock excavation. That study recommended several design criterion for flow modulation and concluded that the percussive jet performance was significantly superior to that of traditional continuous water jets.[2]

Given the positive results of this initial study, SAI began examining the performance and application of percussive jets through a succession of federal research grants.[4, 5] These studies provided valuable insight into the discharge and free-stream dynamics of modulated flows and demonstrated the jet’s propensity of surpassing conventional waterjets in productivity and standoff distance.

In 1993, International Engineering Technology, Inc. (IET) secured an agreement with SAI to continue the development of this technology. Since then, IET has undertaken theoretical and empirical research into the mechanics of percussive modulation, free-stream behavior, and impingement. This work has precipitated in new designs of the physical hardware and instrumentation, a better understanding of the dynamic processes of modulation and bunch formation, and improved insight into the failure mechanisms associated with the impingement of high frequency, quasi-discrete fluid masses.

Research Objectives

The primary objective of this research was to assess the modes of failure associated with the impingement of percussive jets through a controlled series of laboratory experiments. A major component of this investigation was the systematic evaluation of critical modulation and flow parameters relative to rock response. To quantify the key differences between percussive and continuous impingement, this testing methodology also incorporated a comparative analysis that examined the relative performance of comparably powered jets and their sensitivity to specific rock properties. The initial phase of this research was conducted using a medium to course grain biotite granite as the target material. As part of a much larger research program, results of this study were intended to be integrated with those obtained during parametric testing on other rock types in order to serve as the basis for developing a formalized failure criterion and predictive model. Additional elements of this research will be presented in future publications.

RESEARCH METHODOLOGY

In pursuit of these objectives, more than 1,540 kgs of rock specimens were cut using percussive modulated jets as part of a structured testing program. These rock specimens were methodically selected by virtue of their physical attributes and obtained from operating mines and excavation projects with which IET had established ties. While sample preparation and analysis were performed at the Colorado School of Mines, physical testing was conducted at SAI's waterjet laboratory located in Lancaster, California.

The pressurized flow for this testing program was created by a 150 hp KOBE triplex plunger pump (model: Size-4, 180 nominal hp, 15.875 mm diameter plungers). The pump had a prescribed maximum intermittent pressure rating of 206.8 MPa and a theoretical fixed displacement of 27.9 lpm at 370 rpm. For the nozzle diameters employed, the system operating pressures varied between 182.7 to 193.1 MPa, as measured at the pump discharge manifold. As expected, the actual nozzle flow rate at these working pressures was less than the theoretical as a result of inefficiencies and slippage in the pump. Empiric measurements indicated a pump efficiency of somewhere between 75-77% for the fluid pressures used. An analytic estimate of the system's energy (pressure) losses for each component was made over the range of operating parameters used, where the cumulative pressure loss between the pump and the internal annulus of the modulator was approximately 10.0 MPa. An auxiliary feed pump was used to prime the system and maintain a constant fluid pressure of 0.45 MPa at the inlet port of the high pressure pump. The low pressure side of the system also included a 945 liter water storage tank and an inlet line filter.

The flow controls for this system were configured to allow the greatest amount of flexibility in the operation of the flow modulator, with piping efficiency (e.g., pressure losses) viewed as a secondary consideration. Figure 2 shows a schematic diagram of the flow circuit employed. The modulator vessel was connected to the pump accumulator by way of a 3.7 m long, 5.1 mm ID high pressure, flexible hose. The placement of two 3-way, 2-stem manifold valves within the flow circuit provided external control of the modulator assembly. This valving arrangement allowed for independent metering of flow into the modulation vessel and provided unlimited opportunities to dynamically influence flow characteristics as well as modulation frequency and pulse amplitude.

To facilitate jet motion relative to a stationary target, the modulating vessel was securely fastened to a rigid steel structure that housed the traversing mechanism. The traverse possessed two degrees of dynamic freedom in a vertical plane, where a third axis corresponding to the standoff distance could be manually adjusted by changing the position of either the target or the modulator's mount prior to jet operation. Motion was produced by the extension or contraction of two double acting, hydraulic cylinders that linearly actuated the jet's mounting on adjustable slide bearings along two fixed cylindrical supporting rods. To preserve consistency between individual tests, the traverse direction was held constant. Specific traverse velocities were obtained through iterative adjustments in the flow controls and occurred prior to each cutting test to compensate for temperature changes in the hydraulic fluid. The maximum traverse speed that could be repetitively achieved with this particular laboratory setup was 17.8 cm/s and was deemed sufficient for the scope of this study. During testing, a fork lift assembly was used to prop and orient the specimens in front of the traversing jet, where standoff distance between the modulator and the target was gauged using wooden blocks cut to dimension.

The rock samples collected for this study was comprised of a medium to coarse grain biotite granite obtained from a commercial stone quarry near Lyons, Colorado. This granite was highly desirable due to its relatively high strength, low porosity, and lack of appreciable structure. On the basis of acoustic velocity and geomechanical strength, the test specimens prepared from this rock were assumed to be nearly homogeneous and isotropic. As such, they made ideal samples for the purposes of comparative analysis.

Under the testing methodology employed, unconfined rectangular blocks were used to determine the relative effects of surface texture, nozzle diameter, and traverse speed on fragmentation. Individual sample blocks were evaluated in the field relative to an established list of prerequisites outlined in the testing procedures. Great importance was placed on selecting representative samples, given the influence of a rock's structural, mechanical, and petrologic properties on the performance of most waterjet systems. A description of the physical and geomechanical properties of these granite specimens is presented in Table 1.

As each sample block was collected, it was cataloged and sketched, and detailed geologic description was made. This process also entailed the creation of relatively flat, planer surfaces on each sample using diamond saws or hand steels, depending on the intended purpose of the sample. Since the role of surface texture in the fragmentation process was also of interest and a key objective, several specimens required some additional preparation related to polishing and instrumentation. During preparation, portions of select sample blocks were labeled and placed into storage. These representative "splits" served as reference samples and provided specimens for additional geologic investigations, such as petrographic analysis and permeability testing.

Given that this study was conducted over a period of time, it was imperative that changes in the testing apparatus be normalized to a standardized set of specifications prior to each testing session. To do this, jet performance was gauged against a benchmark target for a fixed set of operating conditions. For this study, cement blocks that were cast from the same pour at a local cement company proved to be an ideal target material for this standardization process.

The system operating parameters utilized in this study were selected by virtue of the type of equipment available, the results of previous research, and the established objectives. Since the intended target material was a hard, crystalline rock and the quantity of samples limited, a number of assumptions were made. Foremost among these was that no concerted effort would be made to optimize the jet's excavation efficiency and/or performance for the rock type tested. Since the study objectives could be met without undertaking this arduous task, a strategic decision was made to utilize the maximum volume generated from the available pumping system and to employ nozzle diameters of sufficient size to keep the jet stagnation pressure well above that of the rock's threshold pressure. Table 2 outlines the operating parameters employed during testing, relative to jet type, fluid dynamics, and system variables.

The test strategy was comprised of four fundamental stages, each intending to isolate a specific piece of the overall objective. A primary phase of this research constituted a comparative analysis of the kerfs generated by similarly powered continuous and percussive modulated jets. To mitigate parametric inconsistencies in testing, kerf direction, traverse speed, and rock orientation were held constant for both jets. The kerfs were generated using single and multiple pass configurations, intentionally spaced to minimize the potential for physical interaction between adjacent cuts or the boundary of the sample. The next phase of testing comprised single pass kerfing by a percussive jet at varying traverse speeds. The intent of these particular tests was to establish the time dependent effects of hydropressurization in the rock mass and the efficiency of fracture propagation and macro-erosion as a function of traverse speed. The third test stage concentrated on the impingement of a modulated stream within a preexisting kerf to determine the ability to dilate and extend fractures within the turbulent environment existing inside the kerf. The final stage of testing investigated the influence of surface finish and texture on fragmentation. The intent of this testing phase was two-fold: to examine the effects of surface erosion due to the collapse of fluid bunches during impingement and to determine the role of subsurface fluid penetration in crack propagation.

At the conclusion of every laboratory session, an informal evaluation of the testing methodology, equipment, and observed results was performed. This evaluation proved to be important in providing a cohesive and logical progression of the research over multiple laboratory sessions. Photographs and video were taken of every sample face before, during, and after testing. These images established a visual record of the samples, testing procedures, and experimental results.

As part of the data collection process, the volume, shape, and relief of each kerf was measured and recorded, along with any distinguishing features (e.g. surface exposed fractures and cracks).

Cut volumes and profiles were estimated through a number of different methods depending on geometry and the severity of fragmentation. In addition, measurements were performed by taking cross and longitudinal sections over regularly spaced intervals using depth and inside calipers, a needle micrometer, and dividers. To visually assess the peripheral damage to the rock, each kerf was inspected with a 10 power lens and an oblique light source for cracks, fractures, and other structural discontinuities in the rock fabric. The rock chips and debris ejected during kerfing were also collected and subjected to limited analysis in hopes of correlating particle characteristics (e.g. geometry and size) with apparent failure mechanisms, as well as geologic structure and jet operating parameters.

ANALYSIS OF LABORATORY TESTING

Observed Failure Characteristics

As expected, the cuttings retrieved during percussive jet kerfing indicated that the predominant failure mechanisms involved the initiation, propagation, and/or coalescence of tensile fractures. From these cuttings, it appeared that failure occurred in accordance with criteria common to brittle material fracture. Target surfaces along the cut trajectories exhibited intense spalling with the liberation of convex chips having geometries reminiscent of conventional excavators that employ direct contact tools. A microscopic analysis of these chips showed pristine crystalline faces with little to no indication of shearing action or the proliferation of branch cracking. The mean size of these cuttings were several magnitudes larger than those produced by the comparably powered continuous waterjet. In addition, the size distribution of these cuttings appeared to be substantially greater than those generated by continuous flows, where variability in particle size changed as an inverse function of traverse speed. A visual examination of the largest chip fraction showed evidence that spalling preceded the active cutting face in a manner similar to failure induced by a rolling disc cutter. Many of these chips, however, clearly displayed a kerf structure indicating that the jet was sometimes well within the periphery of the spall prior to it being ejected.

During physical tests conducted with percussive jets, large-scale spalling was often observed with chips extending up to 52 nozzle diameters ahead of the jet/rock interface. Similarly, the breadth of these spalls encompassed one or both sides of the cut trajectory and reached a maximum dimension of 89 nozzle diameters. The difference in magnitude between the maximum and minimum cut widths were on the order of 1,400 percent. These spalling characteristics are quite unique and a radical departure from what is normally observed during continuous waterjet cutting.

Examination of the kerfs generated by percussive modulated jets showed acute pitting (i.e. the removal of individual grains and crystalline masses) along the bottom and sides of the cuts as well as other visual signs of apparent erosion. In many locations, these cavities were conical shaped and deviated at angles divergent to the jet axis. Their extreme prominence and random orientation suggested a preferential mode of attack by the jet on weaker mineral constituents (e.g. biotite) and/or microcracks and discontinuities along crystalline boundaries. In addition, there appeared to be a direct correlation between the occurrence of pitting within the cut floor and localized spalling. Cavities of significant size and depth were routinely observed immediately prior to the generation of large spalls.

A detailed examination of the target surface also revealed a high density of large fractures radiating from the bottom and sides of the cuts. While crack direction proved to be highly erratic, a microscopic investigation showed that they usually emanated from between dissimilar mineral constituents (e.g. quartz and biotite). The fragmentation of individual crystalline elements and the splitting of common minerals were observed but occurred much less frequently. It was also quite evident that a sizable portion of these fractures had experienced some degree of deformation due to dilation and contraction. This conclusion was derived from the existence of secondary radial cracks branching from the exposed, cross-sectional periphery of the primary fractures. In many instances, these fractures extended to free-surfaces, either in the cut or to the rock surface, without the liberation of chips or spalls. The relative length of these fractures sometimes exceeded twice the average cut width and lateral extents up to 6.1 cm. These observations stem from experiments in which crack patterns were identified by injecting fluid into exposed fractures.

Relative Jet Performance

As anticipated, the relative performance of percussive jets was found to be nearly twice as effective as comparably powered, continuous round jets. Table 3 presents a comparative analysis of these two jet types at a traverse velocity of 7.62 cm/s using the same 0.838 mm diameter nozzle. The adjusted percentage difference, as presented in this table, denotes the actual amount of change between percussive and continuous jet performance corrected for variations in nozzle pressure due to frictional and system losses. As calculated, the average difference in adjusted jet productivity was 94.0%. While determined from traverse tests using only 18 data points, the contrast in productivity between these jets was consistent with the results of previous investigations. Of particular interest to this discussion, the cuts produced by continuous waterjets exhibited a greater degree of irregularity than those generated by percussive flows. As measured, the coefficient of variation for continuous jets was higher in cut width (117%) and depth (37%) than their percussive counterparts. Even so, the width-to-depth ratio of the cuts created by these jets was nearly equivalent at 3.9 and 3.7 for continuous and percussive jets, respectively. The amount of time and samples devoted towards quantifying the empiric differences between percussive and continuous jet cutting were intentionally limited as a consequence other testing priorities and the close agreement of the test results with previous research.

Parametric Analysis

Empiric testing demonstrated that cut geometry varied as a function of nozzle diameter and traverse velocity. An analysis of comparably powered percussive jets revealed that a proportional relationship exists between orifice diameter and cut geometry (e.g. depth and width). Similar relationships were also found that correlate these critical parameters to volumetric removal and the rate of excavation (Figures 3 & 4). As these figures clearly indicate, cut geometry proved to be inversely proportional to traverse speed.

Uncharacteristic of continuous waterjet excavation, the average cutting rate for targets with sawed surface textures showed a definitive apex at a traverse velocity of 7.62 cm/s for both nozzle diameters employed (Figure 4). The average cutting rate is calculated by multiplying the average volume removed by the jet's traverse velocity. Continuous jets typically demonstrate linear improvement in volumetric removal and energy efficiency with increases in traverse velocity up until some threshold limit, generally in excess of 100 cm/s.[6] Such proportional relationships were exhibited in percussive cuts made in targets with both polished and rough surface textures. As Figure 6 illustrates, however, this trend did not extend to any of the percussive cutting tests conducted on granite specimens with sawed textures. It is unlikely that this condition is predicated by anomalous data points, since similar path histories over the range of 2.54 to 15.24 cm/s were obtained for different operating parameters and rock types.

From Figure 4, several additional noteworthy observations were made. While the relative magnitude of the peak cutting rate was significantly less for the smaller diameter nozzle, both jet diameters showed substantial improvement in cutting efficiency by increasing the traverse speed above 2.54 cm/s. The overall trend showed a greater incremental increase in performance for the larger diameter jet as traverse speeds varied from 2.54 to 15.24 cm/s. At 2.54 cm/s, the larger jet proved to be 20.8% more efficient than the jet issuing from the smaller nozzle. At 15.24 cm/s, this differential grew to 40.0%, almost a 100% increase. At the apex of the curve (7.62 cm/s), the difference equaled 81.8%. These relationships illustrated that relatively minor increases in traverse velocity could facilitate a nearly four fold increase in cutting performance.

Surface Texture

One of the principle objectives of this testing program was to delineate the influence of target surface finish on jet productivity in hopes that it would lead to a greater understanding of the role of surface fractures and structural imperfections. In the test methodology employed, rock specimens with three different textures were prepared and cut. These textures include polished, diamond sawed, and rough chiseled. Using a constant diameter nozzle of 0.965 mm, rock specimens possessing these different surface finishes were systematically cut utilizing jets at various traverse speeds. The results of this testing phase provided some interesting insight into the role of fluid dispersion and surface penetration in rock failure.

As expected, the influence of the surface finish on jet performance varied as a function of traverse speed. As illustrated in Figure 5, the target surfaces produced with a diamond saw possessed an average rate of volumetric removal (cm^3/cm of cut) far superior to those with rough or polished textures at traverse speeds less than 7.62 cm/s. At the slowest traverse velocity employed (2.54 cm/s), jet productivity on sawed rock surfaces was 93.3% and 107.2% better than that obtained from the rough and polished textures, respectively. Almost linearly, this superiority declined as the traverse velocity increased. Between the nozzle speeds of 2.54 and 7.62 cm/s, jet performance on sawed surfaces dropped over 31%. This decline in efficiency continued until the measured performance of the jet on rough surfaces superseded that of the others at a nozzle speed somewhere near 15.24 cm/s (Figure 6). These trends correlated with the high incidence of spalling that accompanied jet impingement on sawed surfaces at slower traverse velocities. As the nozzle velocity increased above 7.62 cm/s, the frequency and magnitude of these spalling events declined. While the polished texture proved to be the least efficient of those tested, it showed a modest improvement (16.7%) as the traverse velocity was increased from 7.62 to 15.24 cm/s.

As depicted in Figure 6, the average cutting rate increased proportionally for both the rough and polished surfaces with traverse speed, something consistent with continuous jet cutting. While the rate of this increase was substantial for rough textured surfaces, it slowed as traverse speed increased, from 120.0% between 2.54 and 7.62 cm/s to 63.4% between 7.62 and 15.24 cm/s. Conversely, the average cutting rate experienced by percussive jets on the polished rock surface increased from 28.6 to 133.3% over these same traverse intervals.

Cut geometry, relative to average width and depth, displayed similar characteristics to that of volumetric removal, where saw cut surfaces were consistently better than the others at slower traverse speeds. As the traverse velocity increased, cut damage to the rough finished specimens proved to be the best. As before, kerf width and depth were consistently smaller for polished surfaces. For these surfaces, however, the average cut width remained essentially fixed as jet motion increased from 7.62 to 15.24 cm/s.

Multiple Cuts

The intent of traversing a percussive jet several times over the same surface area was to gauge the limiting extent of the jet to propagate fractures within a defined cut and to determine if side-wall loading played any substantive role in kerf expansion. In this experiment, a nozzle diameter of 0.965 mm was used at a constant traverse rate of 7.62 cm/s over samples with a sawed finish. As expected, the total volume of rock removed during cutting increased with each successive pass. The magnitude of this increase, however, jumped significantly from 20% between the first and second passes to 117% between the second and third passes. This unusual trend became pronounced during the calculations of jet productivity. Between the first and second jet passes, a 40.0% decline in cutting rate was realized. In spite of this, a subsequent third pass resulted in a substantial increase in jet productivity (44.4%).

An examination of the average cut width-to-depth ratio, as shown in Figure 7, revealed that little change occurred between the single and two pass cuts (0.2%). A large decline in this ratio (27.1%), however, was observed between the two and three pass cuts. Empirical measurements of the kerfs showed that a substantial percentage of the total volumetric removal after the second jet pass originated from increases in cut depth rather than width. The average cut width remained essentially constant between the two and three pass cuts, varying by only 7.8%. The average cut depth, on the other hand, increased by 26.5% over this same interval.

Another noteworthy observation was that with each successive jet traverse, the coefficient of variance for cut depth decreased, from 41.0% between the first and second passes to 65.2% between the second and third passes. Conversely, there was very little variation in cut width over these intervals, where the actual quantity of change between the first and third passes was negligible.

CONCLUSIONS

The following is a synopsis of the prominent conclusions reached as a consequence of this study.

(1) The modes of failure induced in the crystalline rock type tested were found to be directly dependent upon traverse velocity. Rock failure, at traverse speeds slower than 7.62 cm/s were dominated by the inception and propagation of tensile fractures by hydraulic pressurization. The coalescence of these cracks resulted in intense surface spalling. As traverse speeds increased, the size and prevalence of spalling declined. As nozzle velocities exceeded 7.62 cm/s, failure became dependent upon granular mechanisms associated with differential grain loading, elastic rebound, and surface scouring.

(2) The presence of open surface fractures expedited fluid penetration into the rock mass and augmented the processes facilitating spall development. The role of these surface fractures in failure, however, diminished inversely proportional to traverse speed. At velocities approaching 15.24 cm/s, crack pressurization became subordinate to granular failure processes. This inferred that the fragmentation processes were highly time dependent.

(3) Irregularities in rock surface texture promoted failure mechanisms innate to high velocity traverses. This was ostensibly the result of stress concentrations imparted through the pressurization of residual fluids confined within the surface relief, point loading, and the differential elastic properties of constituents comprising the target material.

(4) Fluid penetration into primary fractures need not be pervasive for crack propagation. The repetitive pressurization of residual fluid by subsequent bunch impacts created transitory point stresses against mineral and structural discontinuities resulting in crack inception. The lateral extension of these tensile flaws required only nominal infiltration of fluid into the crack regime.

(5) In multiple pass configurations, the maximum cut width was reached within two traverses. Once attained, additional jet passes exert little hydraulic stress on the sides of the effected cut, where incremental increases in volumetric removal are solely derived from granular failure in the cut bottom. A limiting depth condition exists most likely due to turbulence and fluid friction/interference within the cut.

(6) Percussive jet productivity was shown to be extremely sensitive to the frequency and magnitude of surface spalling. The proportional decline in jet cutting rate with traverse speed, as witnessed through empiric testing, reflected the transition from tensile to granular failure.

(7) A comparative analysis between percussive and continuous waterjet cutting showed performance differentials consistent with previous research, varying from a few percent to several magnitudes.

ACKNOWLEDGEMENTS

The authors would like to extend their sincere and heartfelt thanks to International Engineering technology, Inc. and Scientific Associates, Inc. for making this study possible. Special gratitude and recognition is due to Dr. Eugene Nebeker, Dr. Song Soo Han, and Mr. Jack Kramer for their technical insight, expertise, and contributions to this work.

REFERENCES

[1] Scientific Associates Inc., Santa Monica, CA, 1978.

[2] Nebeker, E.B., *"Percussive Water Jets for Rapid Excavation"*, Scientific Associates, Inc., Santa Monica, CA., Prepared for the U.S. Army Mobility Equipment Research and Development Center, Contract DAAKOZ-73-C-0163, NTIS No. AD-722931, 1973.

[3] Nebeker, E.B., *"Development of Percussive Water Jets"*, Scientific Associates, Inc., Santa Monica, CA., Prepared for the U.S. Department of Energy, Assistant Secretary for Fossil Energy, Contract No. ET-75-C-01-9094, Final Technical Report, May, 1979.

[4] Nebeker, E.B., *"Percussive Jet Cutting"*, Phase I, Final Report, DOE Contract, Scientific Associates, Inc., Santa Monica, CA., January, 1988.

[5] Summers, D.A., *Waterjetting Technology*, Chapter 7, Section 7.4.2, Chapman & Hall, 1995, pgs 440-442.

NOMENCLATURE

cm/s	centimeters per second
hp	horsepower
ID	internal diameter
kgs	kilograms
lpm	liters per minute
m	meter
mm	millimeters
MPa	megapascal
rpm	revolutions per minute

TABLES

Table 1. Physical Properties of the Rock Specimens

Rock Type	Specific Gravity	Uniaxial Compressive Strength (MPa)	Indirect Tensile Strength (MPa)	Apparent Porosity (%)	Longitudinal Sonic Velocity (1000 m/s)
Biotite Granite	2.7	279.9	12.1	0.9	5.8

Table 2. Fluid Testing Parameters

Jet Types	Percussive		Continuous	
Nozzle Diameter (mm)	0.838	0.965	0.838	0.965
Pump Displacement (lpm)	21.2	21.6	21.2	21.6
Fluid Pressure @ Nozzle (MPa)	172	162	182	172
Nozzle Exit Velocity (m/s)	472	457	485	471
Modulation Frequency (Hz)	18,830	19,260	-	-
Standoff Distance (mm)	108 – 133			
Traverse Velocity (cm/s)	2.54 – 15.24			
Impingement Angle	90˚ (Vertical)			

Table 3. Relative Jet Performance

	Continuous Jet	Percussive Jet	Percent Difference (%)	Adjusted Percent Difference (%)
Ave. Cut Width (mm)	12.95	17.78	73.3	45.2
Ave. Cut Depth (mm)	3.30	4.83	46.2	54.6
Ave. Volumetric Removal (mm^3/mm)	983	1803	83.3	94.0
Ave. Removal Rate (mm^3/s)	2,950	5,410	83.3	94.0

FIGURES

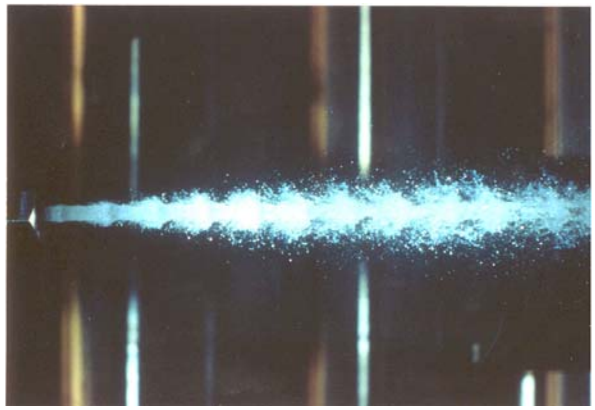

Figure 1. High Speed Photograph of a Percussive Modulated Jet.[1]

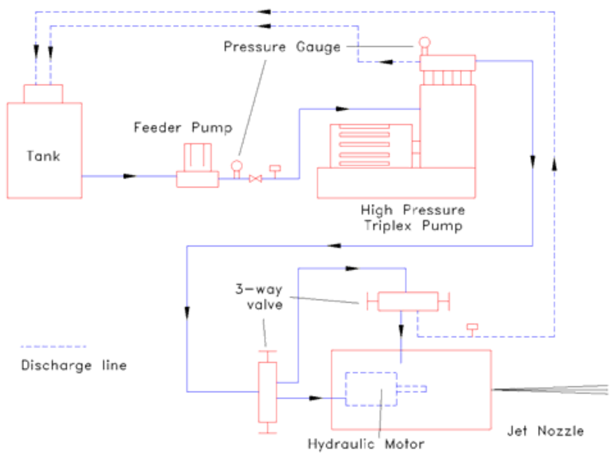

Figure 2. Flow Circuit Schematic.

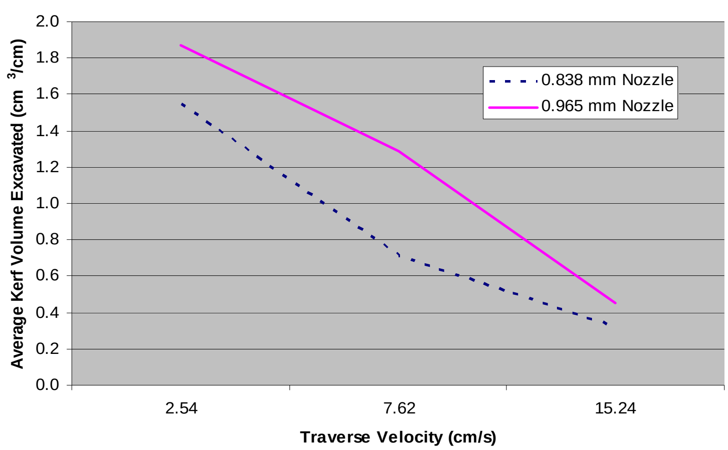

Figure 3. The Effects of Percussive Jet Nozzle Diameter on Volumetric Removal.

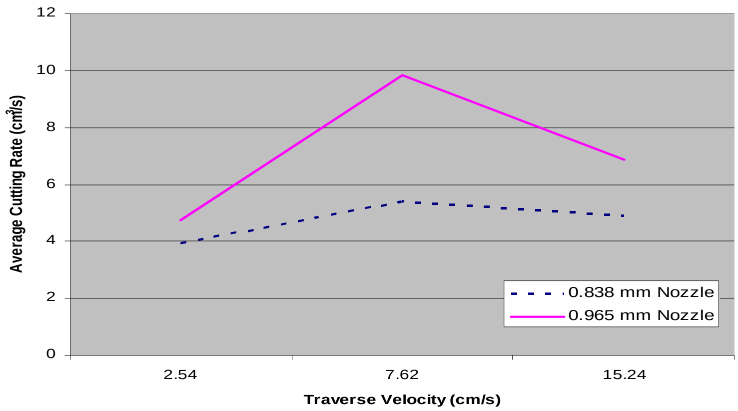

Figure 4. The Effects of Percussive Jet Nozzle Diameter on Cutting Rate.

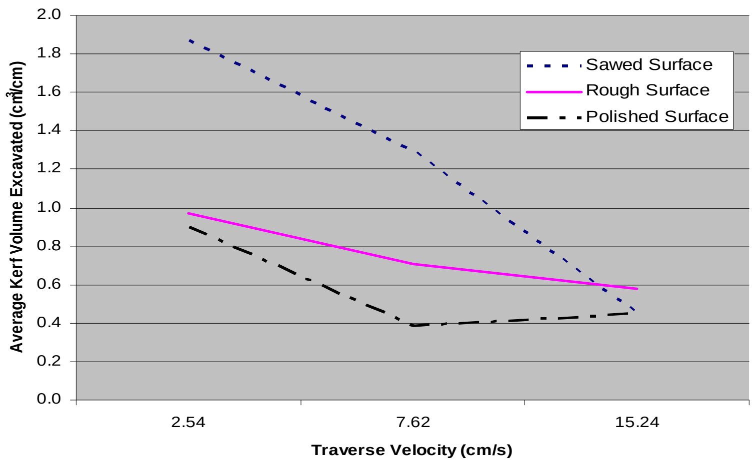

Figure 5. The Effects of Surface Texture on Percussive Jet Volumetric Removal.

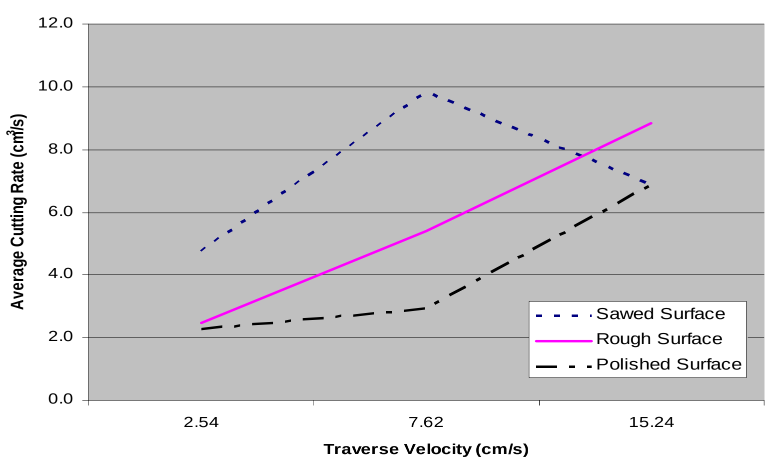

Figure 6. The Effects of Surface Texture on Percussive Jet Cutting Rate.

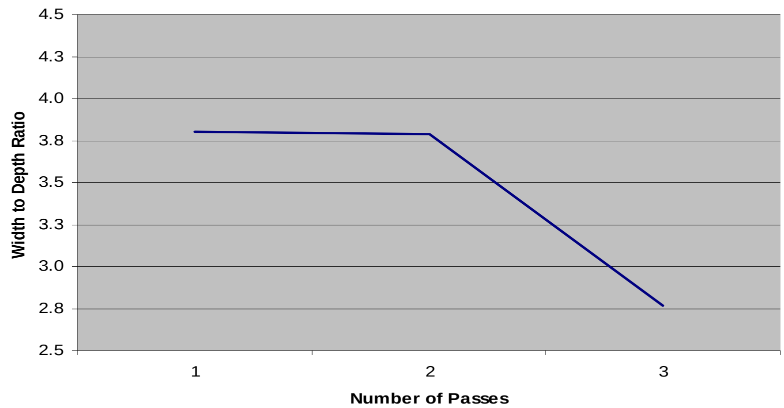

Figure 7. The Cut Width/Depth Ratio for Multiple Passes with a Percussive Jet.